On the evaluation of effective density for plate- and membrane-type acoustic metamaterials without mass attached

Tai-Yun Huang, Chen Shen, and Yun Jing[a)]
Department of Mechanical and Aerospace Engineering, North Carolina State University, Raleigh, North Carolina 27695, USA

(Received 17 March 2016; revised 28 June 2016; accepted 8 July 2016; published online 10 August 2016)

The effective densities of plate- and membrane-type acoustic metamaterials (AMMs) without mass attached are studied theoretically and numerically. Three models, including the analytic model (based on the plate flexural wave equation and the membrane wave equation), approximate model (under the low frequency approximation), and the finite element method (FEM) model, are first used to calculate the acoustic impedance of square and clamped plates or membranes. The effective density is then obtained using the resulting acoustic impedance and a lumped model. Pressure transmission coefficients of the AMMs are computed using the obtained densities. The effect of the loss from the plate is also taken into account. Results from different models are compared and good agreement is found, particularly between the analytic model and the FEM model. The approximate model is less accurate when the frequency of interest is above the first resonance frequency of the plate or membrane. The approximate model, however, provides simple formulae to predict the effective densities of plate- or membrane-type AMMs and is accurate for the negative density frequency region. The methods presented in this paper are useful in designing AMMs for manipulating acoustic waves. © *2016 Acoustical Society of America*. [http://dx.doi.org/10.1121/1.4960590]

[MRH] Pages: 908–916

I. INTRODUCTION

The theoretical and experimental investigations of acoustic metamaterials (AMMs) have opened up numerous fascinating possibilities in recent years,[1,2] such as negative refraction,[3,4] subwavelength imaging[5] and cloaking.[6] One of the crucial requirements for the realization of these applications is to have negative effective parameters. For instance, a great amount of effort has been made to design a material that exhibits negative density. These AMMs have been used to achieve superlensing,[7,8] partial focusing,[9,10] cancelling out aberrating layers,[11] and noise reduction.[12–14] Liu *et al.* pioneered the realization of locally resonant acoustic metamaterials with negative density in 2000 (Ref. 15). This structure consisted of a dense core with a soft elastic coating, both embedded in a matrix material. Yang *et al.* proposed a different type of locally resonant materials by attaching a small mass to an elastic membrane.[16] Near the anti-resonance frequency, the effective density was shown to be negative and the sound transmission can be orders of magnitude lower than that given by the mass law. The effective density was reported to be negative over a narrow band. Naify *et al.* studied the influence of the membrane and mass properties using the finite element method (FEM) and validated the results experimentally.[17] In their later work, the behavior of multiple units with the effects of non-uniform mass distribution and frame compliance were examined.[18] For the typical configuration of locally resonant membrane-type AMMs, although the attached mass serves as a means to tuning the eigenfrequencies, it introduces negative density in a rather narrow-band frequency and the associated damping could be strong.[19] It was verified later that the tension from the membrane alone is able to give rise to negative density and the non-resonance membrane-type AMMs were demonstrated by Lee *et al.*[20,21] Shortly after, it was discovered that clamped plates can produce similar results.[22]

The idea of using membranes or plates without mass attached for achieving negative density has attracted a lot of attention due to the simple structure and outstanding effectiveness. The effective density of membrane- and plate-type AMMs is negative below a cutoff frequency (the first resonance frequency of the plate or membrane),[22] which means it is a broadband phenomenon if designed properly. Another intriguing property of membrane- or plate-type AMMs without mass attached is that the effective density is near zero around the cutoff frequency,[23] implying that the phase undergoes little changes within the AMMs. It was demonstrated that the density-near-zero metamaterial can be used in extraordinary transmission,[24,25] sound tunneling,[26] and subwavelength imaging.[26,27]

To use plate- or membrane-type AMMs for designing devices controlling acoustic waves, it is critically important to know exactly the effective density for a given AMM structure. For example, in designing complimentary metamaterials (CMMs),[11] the effective density needs to be tuned to a certain value in order to perfectly cancel out the unwanted aberrating layer. Although the effective density of an AMM based on circular plates can be calculated using a lumped model,[28] no explicit derivation of effective density has been reported for square membranes and plates, which were

[a)]Electronic mail: yjing2@ncsu.edu

 0001-4966/2016/140(2)/908/9/$30.00

used in recent studies.[9,11] This paper aims to theoretically and numerically investigate the membrane- and plate-type AMMs without mass attached. The acoustic impedances of square plates and membranes under uniform acoustic pressure are first computed. This is accomplished by three different approaches: analytic models, approximate models, and FEM. The effective density can be then estimated for plate- and membrane-type AMMs using the lumped model. The paper is structured as follows: in Sec. II, the acoustic impedance of a plate is evaluated by three different methods and the corresponding effective density and sound transmission of the plate-type AMM are obtained afterwards. In Sec. III, a similar analysis is carried out for membrane-type AMMs. Section IV concludes the paper.

II. PLATE-TYPE ACOUSTIC METAMATERIALS WITHOUT MASS ATTACHED

A. Analytic model for the acoustic impedance of a square, clamped plate

Although this section focuses on square plates as they have been used recently for building two dimensional (2D) negative density CMMs,[11] the analytic model presented here is generic and can be readily used for rectangular plates. The analytic approach presented here is similar to that in Ref. 29, in which the plate vibration under point forces, couples and piezomoments were studied. For a thin, clamped plate under a net sound pressure $P(x,y,t)$, the governing equation of the transverse displacement $W(x,y,t)$ is the flexural wave equation which reads

$$D\nabla^4 W(x,y,t) + \rho h \frac{\partial^2 W(x,y,t)}{\partial t^2} = P(x,y,t), \tag{1}$$

where D is the flexural rigidity and $D = Eh^3/12(1-\nu^2)$; E, ν, ρ, and h are the Young's modulus, Poisson's ratio, density and thickness of the plate, respectively.

Assuming harmonic excitations with angular frequency ω, $P(x,y,t)$, and $W(x,y,t)$ can be written as

$$P(x,y,t) = p(x,y)e^{j\omega t}, \quad W(x,y,t) = w(x,y)e^{j\omega t}, \tag{2}$$

$p(x,y)$ and $w(x,y)$ can be expanded by eigenfunctions as

$$p(x,y) = \sum_{m=1}^{\infty}\sum_{n=1}^{\infty} p_{mn}\varphi_{mn}(x,y),$$
$$w(x,y) = \sum_{m=1}^{\infty}\sum_{n=1}^{\infty} w_{mn}\varphi_{mn}(x,y), \tag{3}$$

where $\varphi_{mn}(x,y)$ can be further decomposed using the separation of variables, i.e., $\varphi_{mn}(x,y) = X_m(x)Y_n(y)$. $X_m(x)$ and $Y_n(y)$ are chosen to be the same as the eigenfunctions for a beam clamped on both ends to satisfy the clamped boundary condition (the transverse displacement and slope of plate are zero) and the equation of motion for the plate. They are given by

$$X_m(x) = J\left(\frac{\lambda_m x}{a}\right) - \left[\frac{J(\lambda_m)}{H(\lambda_m)}\right] H\left(\frac{\lambda_m x}{a}\right),$$
$$Y_n(y) = J\left(\frac{\lambda_n y}{a}\right) - \left[\frac{J(\lambda_n)}{H(\lambda_n)}\right] H\left(\frac{\lambda_n y}{a}\right), \tag{4}$$

where a is the width of the square plate, $J(u) = \cosh(u) - \cos(u)$, $H(u) = \sinh(u) - \sin(u)$. λ_m or λ_n satisfies the equation $\cosh(\lambda)\cos(\lambda) = 1$.

Combining Eqs. (2)–(4), $P(x,y,t)$ and $W(x,y,t)$ can be obtained and substituted into Eq. (1), w_{mn} can be then written as

$$w_{mn} = \frac{\int_0^a\int_0^a p(x,y)X_m Y_n dxdy}{D(I_1I_2 + 2I_3I_4 + I_5I_6) - \rho h\omega^2 I_2 I_6}, \tag{5}$$

where $I_1 = \int_0^a X_m^{(4)} X_m dx$, $I_2 = \int_0^a Y_n^2 dy$, $I_3 = \int_0^a X_m'' X_m dy$, $I_4 = \int_0^a Y_n'' Y_n dy$, $I_5 = \int_0^a Y_n{}^{(4)} Y_n dy$, $I_6 = \int_0^a {X_m}^2 dx$, and the superscript in "()" indicates the order of the derivative and double prime is the second order derivative.

At the resonance frequencies, w_{mn} reaches infinity in the absence of damping. The resonance angular frequencies can thus be obtained by setting the denominator of Eq. (5) to zero, which leads to

$$\omega_{mn} = \sqrt{\frac{D(I_1I_2 + 2I_3I_4 + I_5I_6)}{\rho h I_2 I_6}}. \tag{6}$$

The acoustic impedance of a vibrating plate is defined as

$$Z_{am} = \frac{\int_0^a\int_0^a P(x,y,t)dxdy}{\bar{V}(t)a^4} = \frac{\int_0^a\int_0^a P(x,y,t)dxdy}{\frac{\partial \bar{W}(t)}{\partial t}a^4}$$
$$= \frac{\int_0^a\int_0^a p(x,y)dxdy}{j\omega\bar{w}a^4}, \tag{7}$$

where $\bar{V}$, $\bar{W}$, and $\bar{w}$ are the average velocity, transverse displacement, and magnitude of transverse displacement, respectively.Consider a subwavelength size waveguide [Fig. 1(a)], plane waves with normal incidence angle can be assumed. $p(x,y)$ is, therefore, a constant p_0 (uniform distribution) and Eq. (7) becomes

$$Z_{am} = \frac{1}{j\omega\int_0^a\int_0^a\left[\sum_{m=1}^{\infty}\sum_{n=1}^{\infty}\frac{\int_0^a\int_0^a X_m Y_n dxdy}{D(I_1I_2 + 2I_3I_4 + I_5I_6) - \rho h\omega^2 I_2 I_6} X_m Y_n\right]dxdy}. \tag{8}$$

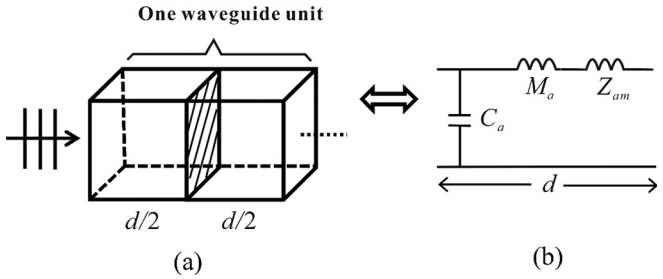

FIG. 1. (a) Schematic of a single unit cell with a length d for plate- or membrane-type AMMs without mass attached. (b) The lumped model for plate- or membrane type AMMs. Z_{am} represents the acoustic impedance of the plate or membrane.

Equation (8) is computed numerically using Matlab. Specifically, the Simpson's 3/8 rule is applied to approximate the integrals.

B. Approximate model for the acoustic impedance of a square, clamped plate

The acoustic impedance Z_{am} of a plate can be divided into two parts at low frequencies (frequency around or below the first resonance frequency of the plate). They are the acoustic compliance (C_{am}) and acoustic mass (M_{am}) in the lumped model[28] [Fig. 1(b)]. In other words,

$$Z_{am} = \frac{1}{j\omega C_{am}} + j\omega M_{am}. \tag{9}$$

When the frequency of interest is significantly below the first resonance frequency of the plate, the acoustic compliance term will dominate and the acoustic mass term can be ignored. Therefore, C_{am} can be determined by computing Z_{am} at an extremely low frequency using Eq. (9). Similar to circular plates, it is assumed that the acoustic compliance is associated with the dimensions and flexural rigidity.[28] By equating the unit of Z_{am} ($\mathrm{kg/m^4s}$) and the unit of the term containing C_{am} ($1/j\omega C_{am}$) in Eq. (9), the unit of C_{am} is calculated to be $\mathrm{m^4s^2/kg}$. Consequently, the power for D ($\mathrm{kgm^2/s^2}$) must be -1 and the power for a (m) must be 6. The formula for C_{am} is found to be

$$C_{am} = 3.73 \times 10^{-4} \frac{a^6}{D}. \tag{10}$$

Note that Z_{am} should be zero at the first resonant frequency (ω_{11}) of the plate. Hence, M_{am} can be analytically obtained from Eq. (9) as

$$M_{am} = \frac{1}{{\omega_{11}}^2 C_{am}}, \tag{11}$$

where $\omega_{11} = (C_0/a^2)\sqrt{D/\rho h}$ and C_0 is a constant.[30] Substituting Eq. (10) into Eq. (11) yields

$$M_{am} = \frac{1}{3.73 \times 10^{-4} {C_0}^2} \frac{\rho h}{a^2} = C_1 \frac{\rho h}{a^2}. \tag{12}$$

To determine the constant C_1, ω_{11} is first computed using the analytic model [Eq. (6)] for a random plate, M_{am} can then be calculated using Eq. (11) since both C_{am} and ω_{11} are known. Finally, C_1 is determined from Eq. (12). Since C_1 is independent of the dimensions and properties of the plate, the obtained C_1 is general and it is found that

$$M_{am} = 2.06 \frac{\rho h}{a^2}. \tag{13}$$

Equations (10) and (13) provide the acoustic compliance and acoustic mass for the approximate model to predict the acoustic impedance for a square, clamped, thin plate. It is noted that the acoustic compliance is proportional to a^6 for square plates whereas it is proportional to r^6 (r being the radius) for circular plates.[28]

C. FEM model for the acoustic impedance of a square, clamped plate

To verify the analytic and approximate models, a commercial FEM package COMSOL is adopted to analyze the vibration of a clamped plate under a certain surface pressure. The solid-acoustic interaction module is used. As indicated by Eq. (7), the acoustic impedance of the plate, Z_{am}, can be extrapolated using the average surface velocity and the net pressure on the plate obtained from the FEM simulation. Two distinct FEM models are used to achieve this goal. In the first model, a boundary load is directly applied on the top surface of the clamped plate. The net pressure is therefore F/a^2, where the F is force in Newton. In the second model, a waveguide is created where clamped plates are placed inside in a periodical manner [Fig. 1(a)]. A plane wave enters from one side and the end of the waveguide is set up to be a non-reflecting boundary. The acoustic pressures on two planes extremely close to the plate are obtained in order to compute the net pressure. These two models are denoted the FEM-boundary model and FEM-waveguide model, respectively. For both FEM models, convergence studies are carried out in order to ensure most accurate results.

Consider a rubber plate ($E = 10\,\mathrm{MPa}$, $\nu = 0.49$ and $\rho = 1000\,\mathrm{kg/m^3}$) with dimensions $a = 10\,\mathrm{mm}$ and $h = 0.1\,\mathrm{mm}$ as a study case. The first resonance frequency of this plate is at around 190 Hz. The length of the unit cell is 2 mm. The acoustic impedance can be calculated using the three different methods presented above. Since in the FEM-waveguide model, the plate number can be varied. We first examine whether the number of plates (units) would change the calculated acoustic impedance. Figure 2 illustrates the acoustic impedance obtained from the FEM-waveguide model with various numbers of units. Only the imaginary part of the acoustic impedance is shown since the real part is zero. Due to the large computation, the maximum unit number considered here is three. In all three simulations, the acoustic impedance is extracted for the first plate in the waveguide. However, additional simulations show that the acoustic impedances extracted from other plates (the second and the third plate) are almost identical.

Figure 2 indicates that having multiple waveguide units will not significantly affect the acoustic impedance of a plate. This result is expected because the same plate with the same boundary condition should have identical acoustic

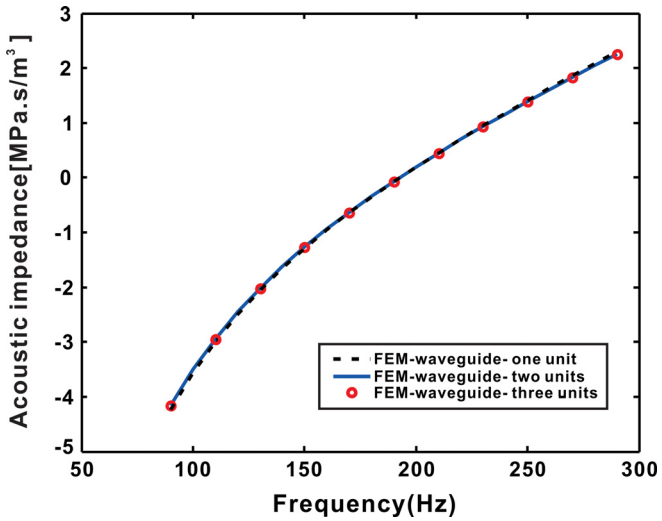

FIG. 2. (Color online) The acoustic impedances predicted by the FEM waveguide model with one, two, and three unit cells, respectively.

impedance as long as the excitation conditions (uniform pressure on the plate) are also the same.

Figure 3 shows the comparison among different models for the acoustic impedance. One can observe slight discrepancy between the analytic and simulation (FEM) results, which is possibly caused by the approximations in the flexural wave equation for a thin plate and inevitable numerical errors in FEM. Because the lumped model is accurate only around and below the resonance frequency,[28] the approximate model becomes less accurate when the frequency is significantly higher than the resonance frequency (190 Hz). At low frequencies, the approximate model agrees very well with the analytic model. Around the resonance frequency, the acoustic impedance is near zero, as expected. The phase difference between the net pressure on the plate and vibrating velocity changes by 180° as the frequency transitions from below ω_{11} to above ω_{11}, so that the impedance transitions from being negative to positive.

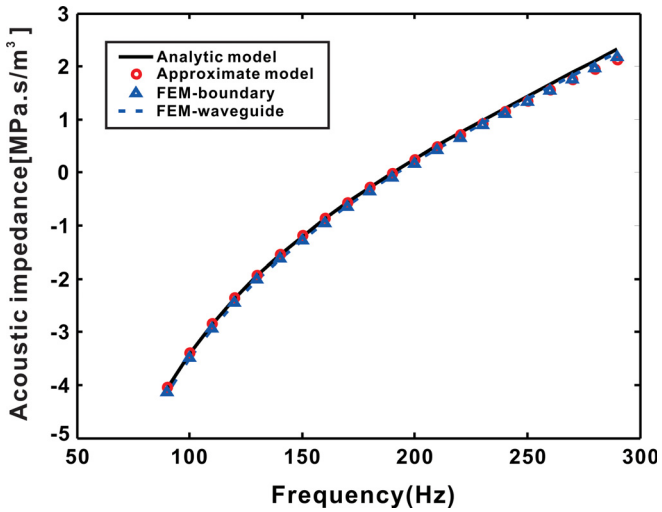

FIG. 3. (Color online) The acoustic impedances predicted by the analytic model, approximate model, FEM-boundary model, and FEM-waveguide model.

D. Effective density

Since the wavelength of the incident sound wave is much larger than the unit size, the AMM [Fig. 1(a)] can be regarded as an effective homogeneous media whose effective density ρ_{eff} can be evaluated. Under the low frequency approximation, the lumped model[28] [Fig. 1(b)] can be employed to predict the effective density of the AMMs. The acoustic medium can be approximated by a shunt acoustic compliance (C_a) and a series acoustic mass (M_a), which are given by

$$M_a = \frac{\rho_0}{a^2} d, \quad C_a = \frac{a^2}{K} d, \tag{14}$$

where ρ_0 is the density of the acoustic medium and is chosen as air ($1.2\,\text{kg/m}^3$) in this study; K is the bulk modulus of the acoustic medium and d is the length of a unit cell assuming the thickness of the plate/membrane is negligible. Otherwise the length of the unit cell is $d + h$. When the rubber plate vibrates, the surrounding acoustic medium will behave like added mass to resist the vibration so that Z_{am} is in series with M_a.

The effective density (ρ_{eff}) of this waveguide unit can be obtained as[28]

$$\rho_{\text{eff}} = \frac{(j\omega M_a + Z_{am})a^2}{j\omega d}. \tag{15}$$

Substituting Eqs. (9), (10), (13), and (14) into Eq. (15), an approximate model for predicting the effective density can be established and the equation reads

$$\rho_{\text{eff}} = \rho_0 - \frac{2.68 \times 10^3 D}{\omega^2 a^4 d} + \frac{2.06\rho h}{d}. \tag{16}$$

To verify the accuracy of the lumped model, a finite-difference approximation method[11,22,31] is used to retrieve the effective density for the structure shown in Fig. 1(a). In this approach, the FEM is first used to compute the sound field in the waveguide and the calculated pressure and velocity are used to estimate the effective density. This approach is denoted the FEM-finite difference approach. Starting from the 1D Euler's equation, the pressure p and the velocity v are related by

$$\frac{dp}{dx} = -j\omega\rho_{\text{eff}} v. \tag{17}$$

Assuming the unit cell size is considerably smaller than one wavelength, Eq. (17) can be rewritten using the finite-difference approximation as

$$\frac{\Delta p}{d} = -j\omega\rho_{\text{eff}} \bar{V}, \tag{18}$$

where $\Delta p = p_1 - p_2$; p_1 and p_2 are the pressures at the right end and left end of the unit cell, respectively; $\bar{V}$ is the average transverse velocity on the plate. By using Δp and $\bar{V}$ obtained from FEM simulations, the effective density can be calculated as

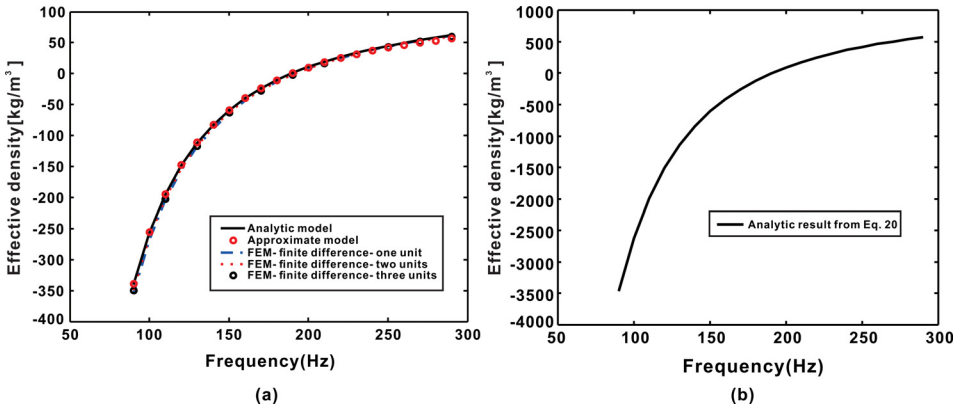

FIG. 4. (Color online) The effective density of the plate-type AMM. (a) Results produced from three different models. (b) Results predicted from Eq. (20).

$$\rho_{\text{eff}} = \frac{\Delta p}{d}\frac{j}{\omega \bar{V}}. \tag{19}$$

Figure 4(a) shows the effective density predicted by the analytic model, approximate model, and the FEM-finite difference model. Only the real part of the density is shown as the imaginary part is negligible (exactly equal to zero in the analytic and approximate models). For the FEM-finite difference model, the number of unit cells varies from one to three. Similar to the acoustic impedance case, no significant change is observed. The analytic and approximate models agree well with the FEM-finite difference model. The slight discrepancy is expected as they do not produce exactly the same acoustic impedance as that predicted by the FEM models (Fig. 3). When the frequency is below the first resonance frequency of the square clamped plate (around 190 Hz), the effective density is negative. This is because the velocity is 90° out of phase with the acceleration (a) and therefore the acceleration is 180° out of phase with the pressure/force (F). By forcing the Newton's second law $F = ma$, m must be negative. When the frequency is above the first resonance frequency, the unit vibrates reversely (180° phase change) and the net pressure on the unit is in phase with the vibrational acceleration of the plate and the effective density becomes positive. It is worthwhile to mention that, a simple equation has been proposed to predict the effective density of plate- or membrane-type AMMs without mass attached, which reads[22]

$$\rho'_{\text{eff}} = \rho\left(1 - \frac{{\omega_c}^2}{\omega^2}\right). \tag{20}$$

This equation, however, predicts the effective density of the vibrating plate or membrane alone without considering the fluid in the waveguide, whereas we took both the plate and the fluid in the waveguide into account and treated them as a homogenized medium to evaluate the effective density. The effective density predicted by Eq. (20) can be seen in Fig. 4(b), which is dramatically different from those in Fig. 4(a), although they both show near-zero density around the resonance frequency.

The next case considers the effect of damping of the plate. The damping is taken into account *ad hoc* by considering a loss factor α so that the Young's modulus of the plate becomes a complex number, i.e., $E' = E(1 + j\alpha)$. This E' is used to calculate the flexural rigidity D, which further leads to the acoustic impedance and the effective density using Eqs. (15) and (16). Two values of frequency independent loss factor are considered, i.e., 0.1 and 0.3. The real part of effective density, shown in Fig. 5(a), remains the same as the case without considering the damping. As the loss factor increases, the magnitude of the imaginary part of effective density also increases as shown in Fig. 5(b). In addition, the imaginary part of the effective density is always negative which introduces further energy loss to the sound transmission. It is noted that the sign of the imaginary part of the density depends on whether $e^{j\omega t}$ or $e^{-j\omega t}$ is used. In the cases studied, the imaginary part of the density is on the same order to the real part of the density, therefore the damping effect cannot be ignored for α on the order of 0.1, which is common for polymeric materials.

To further validate the predicted effective density, transmission coefficients through plate-type AMMs are also

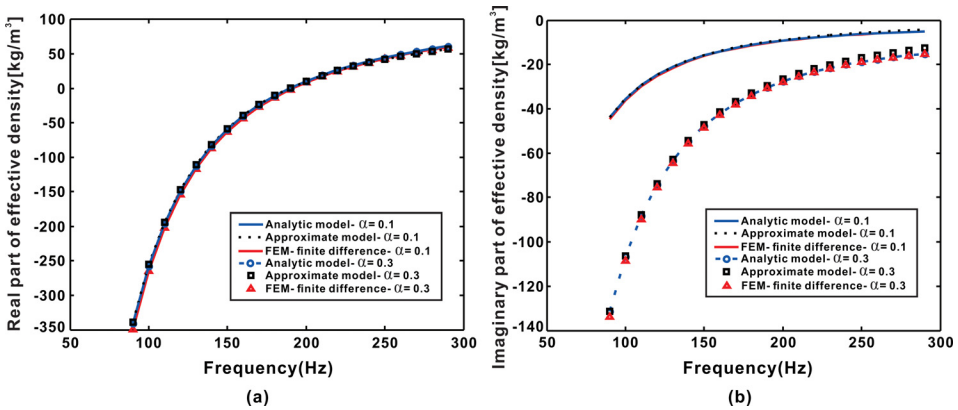

FIG. 5. (Color online) The effect of the loss factor α on the effective density. α is chosen as 0.1 and 0.3. (a) Real part of the effective density. (b) Imaginary part of the effective density.

computed and compared among different models. The pressure reflection and transmission coefficients through a homogeneous medium are given by[32]

$$R = \frac{{Z_m}^2 - {Z_0}^2}{{Z_0}^2 + {Z_m}^2 + 2jZ_0Z_m\cot(\phi)},$$
$$T = \frac{1+R}{\cos(\phi) - \frac{Z_m j\sin(\phi)}{Z_0}}, \quad (21)$$

where $Z_m(=\rho_{\text{eff}}c_{\text{eff}})$ is the characteristic impedance of the waveguide. $c_{\text{eff}} = \sqrt{B_{\text{eff}}/\rho_{\text{eff}}}$, where B_{eff} is the effective bulk modulus and c_{eff} is the effective speed of sound. It was shown that membranes/plates in the waveguide do not alter the effective bulk modulus of the medium so that B_{eff} is the same as the bulk modulus of air.[33] However, it should be kept in mind that, this is not strictly true for all cases. For instance, if the waveguide is largely composed of membranes/plates in volume, or if the background medium is something other than air, the modulus of membranes/plates may have a non-trivial effect on B_{eff}. $Z_0 = \rho_0 c_0$ is the characteristic impedance of the air. $\phi = -2\pi fnd/c_{\text{eff}}$ is the phase change of the sound through the medium where n is the number of unit cells and nd is the total length of the AMM. If the plate thickness h is not negligible, d has to be replaced by $d+h$.

Using the ρ_{eff} predicted from the analytic and approximate models, the transmission coefficients of the plate-type AMMs can be calculated. To verify the results, the transmission coefficients are directly computed using FEM. Figure 6 shows the transmission coefficient of a three unit plate-type AMM. Figure 6(a) shows the results without considering the damping whereas Fig. 6(b) shows the results with damping. Three different models agree very well over the frequency range under consideration. This also indicates that the presence of the plates indeed does not change the bulk modulus as assumed earlier. When there is no damping, the transmission coefficients reach the peak (1.0) at the resonance frequency as expected. With the presence of the damping, the transmission coefficients are reduced due to the energy loss in the plate. In both cases, the approximate model becomes less accurate at a frequency significantly higher than the resonance frequency.

III. EFFECTIVE DENSITY OF MEMBRANE-TYPE ACOUSTIC METAMATERIALS WITHOUT MASS ATTACHED

This section focuses on the membrane-type AMMs. Similarly, the analytic model, approximate model, and the FEM model are developed to predict the acoustic impedance as well as the effective density.

A. Analytic model for the acoustic impedance of a square, clamped membrane

The governing equation of the transverse displacement $W_1(x,y,t)$ of a pre-stretched membrane under the net pressure $P_1(x,y,t)$ is[34]

$$T_1\nabla^2 W_1(x,y,t) - \rho_1 h_1 \frac{\partial^2 W_1(x,y,t)}{\partial t^2} = -P_1(x,y,t), \quad (22)$$

where T_1 is the uniform tension per unit length; ρ_1 and h_1 are the density and thickness of the membrane, respectively.

Assuming time-harmonic solutions, i.e., $P_1(x,y,t) = p_1(x,y)e^{j\omega t}$, $W_1(x,y,t) = w_1(x,y)e^{j\omega t}$, Eq. (22) leads to

$$\nabla^2 w_1(x,y) + \beta^2 w_1(x,y) = -\frac{p_1(x,y)}{T_1}, \quad (23)$$

where $\beta = \omega\sqrt{\rho_1/T_1}$ is the wavenumber of the transverse wave on the membrane.

The eigenfunction of a clamped square membrane is well-known as[34]

$$\varphi_{1mn}(x,y) = A_1A_3\sin\left(\frac{m\pi x}{a}\right)\sin\left(\frac{n\pi y}{a}\right). \quad (24)$$

After normalization, $A_1A_3 = 2/\sqrt{\rho_1 a^2}$.

The resonance angular frequencies can be readily derived as[34]

$$\omega_{mn} = \frac{\pi}{a}\sqrt{\frac{T_1}{\rho_1}(m^2+n^2)}. \quad (25)$$

$w_1(x,y)$ and $p_1(x,y)$ can be expanded using $\varphi_{1mn}(x,y)$ as

$$p_1(x,y) = \sum_{m=1}^{\infty}\sum_{n=1}^{\infty} Q_{mn}\varphi_{1mn}(x,y),$$
$$w_1(x,y) = \sum_{m=1}^{\infty}\sum_{n=1}^{\infty} w_{1mn}\varphi_{1mn}(x,y). \quad (26)$$

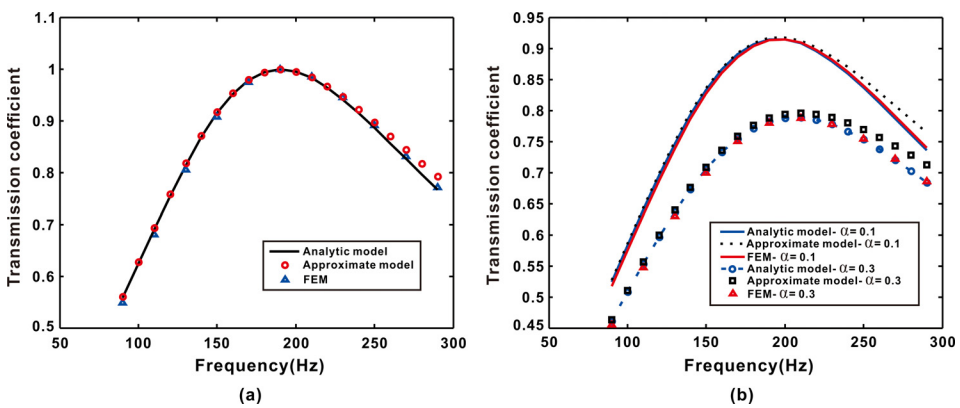

FIG. 6. (Color online) The transmission coefficient of the plate-type AMM with three unit cells. (a) Without considering the loss. (b) With loss factor α: 0.1 and 0.3.

Substituting Eq. (26) into Eq. (23), w_{1mn} can be shown as

$$w_{1mn} = \frac{1}{T_1}\frac{Q_{mn}}{\beta_{mn}{}^2 - \beta^2}, \tag{27}$$

where $\beta_{mn} = \omega_{mn}\sqrt{\rho_1/T_1}$ and $Q_{mn} = \int_0^a \int_0^a \rho_1 h_1 p_1(x,y)\varphi_{1mn}(x,y)dxdy$.

Similar to the case of plate-type AMMs in waveguides, plane waves are assumed and $p_1(x,y) = p_0$ and Q_{mn} becomes

$$\begin{aligned} Q_{mn} &= \frac{2h_1 p_0\sqrt{\rho_1}}{a}\int_0^a\int_0^a \sin\left(\frac{m\pi x}{a}\right)\sin\left(\frac{n\pi y}{a}\right)dxdy \\ &= \frac{2h_1 p_0 a\sqrt{\rho_1}}{mn\pi^2}\left[1-(-1)^m\right]\left[1-(-1)^n\right]. \end{aligned} \tag{28}$$

Combining Eqs. (27) and (28) and then substituting the resulting equation of w_{1mn} into Eq. (26), $w_1(x,y)$ can be obtained as

$$\begin{aligned} w_1(x,y) = \sum_{m=1}^{\infty}\sum_{n=1}^{\infty} &\frac{4p_0}{\rho_1 h_1(\omega_{mn}{}^2 - \omega^2)mn\pi^2}\left[1-(-1)^m\right] \\ &\times\left[1-(-1)^n\right]\sin\left(\frac{m\pi x}{a}\right)\sin\left(\frac{n\pi y}{a}\right). \end{aligned} \tag{29}$$

Substituting Eq. (29) into Eq. (7), the acoustic impedance of a clamped square membrane is analytically written as

$$Z_{am1} = \frac{1}{j\omega a^2\sum_{m=1}^{\infty}\sum_{n=1}^{\infty}\frac{4}{\rho_1 h_1(\omega_{mn}{}^2-\omega^2)m^2n^2\pi^4}\left[1-(-1)^m\right]^2\left[1-(-1)^n\right]^2}. \tag{30}$$

The summations are calculated numerically. Clearly, even number modes (m, $n = 2, 4, 6,\ldots$) do not contribute to the acoustic impedance, because the uniform pressure on the membrane does not excite those modes.

In contrast to plates, the acoustic impedance of the clamped membranes does not relate to the flexural rigidity (D) but rather the pre-stretched tension (T_1). The membrane model is only valid if the thickness is significantly smaller than the width and the tension is sufficiently large so that the effect of the tension dominates over that of the elasticity of the membrane.

B. Approximate model for the effective density of a square, clamped membrane

Similar to the case of plates, an approximate model for the acoustic impedance of clamped, square membranes can be derived and the acoustic compliance and mass are

$$M_{am1} = 1.44\frac{\rho_1 h_1}{a^2}, \quad C_{am1} = 0.035\frac{a^4}{T_1}. \tag{31}$$

To verify the analytic and approximate model for the acoustic impedance, the two FEM models are again used for verification. Figure 7 shows the results for the case where $a = 10\,\text{mm}$, $h_1 = 35\,\mu\text{m}$, $T_1 = 2\,\text{MPa}$, and $d = 2\,\text{mm}$ (this number d is only used in the FEM waveguide model when there are multiple membranes).

Similar to plates, only the imaginary part of the impedance is shown here. The acoustic impedance of the membrane is zero at the first resonance frequency (around 3162 Hz in this case) and is negative below that frequency. The analytic and the two FEM models agree well throughout the entire frequency range. The approximate model becomes less accurate at frequencies above the resonance frequency.

The damping effect is not studied here for membranes because it is expected to be negligible since the thickness is extremely small. However, it is still possible to force the damping by using a complex number for the tension.

C. Effective density

After obtaining the acoustic impedance, the effective density can then be calculated by using Eq. (15). Substituting Eq. (31) into Eq. (15), the equation for predicting the effective density from the approximate model reads

$$\rho_{\text{eff1}} = \rho_0 - \frac{28.57T_1}{\omega^2 a^2 d} + \frac{1.44\rho_1 h_1}{d}. \tag{32}$$

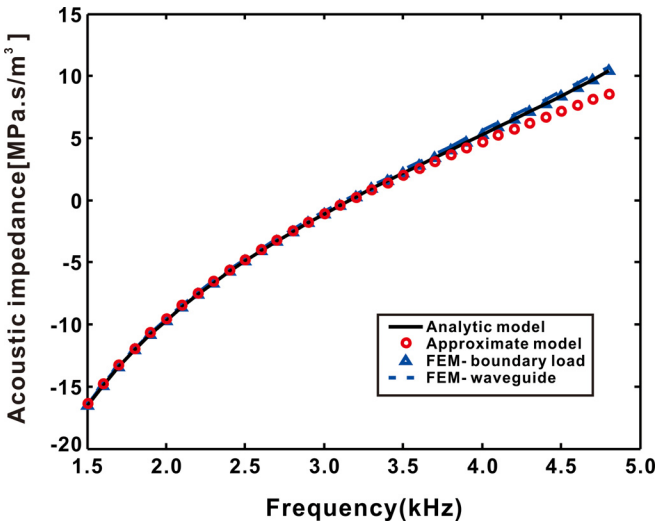

FIG. 7. (Color online) The acoustic impedance of a clamped square membrane predicted by the analytic model, approximate model, FEM-boundary model, and FEM-waveguide model.

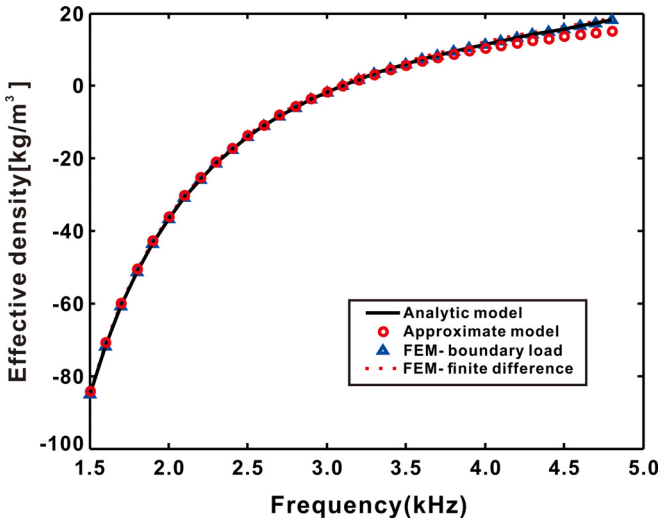

FIG. 8. (Color online) The effective density of the membrane-type AMM.

Figure 8 presents the effective density predicted by the three different approaches. The FEM-finite difference approach is used to verify the analytic and approximate models. All models agree well below the resonance frequency. Similar to the plate-type acoustic metamaterial, the approximate model is less accurate above the resonance frequency. However, the approximate model could still be useful because the frequency of interest is typically below the resonance frequency where the effective density is negative.

Since for square, clamped membranes, a closed form solution for the displacement can be found, the analytic model is expected to be more accurate than that of plates. Finally, Fig. 9 illustrates the sound transmission coefficient for the membrane-type AMM as shown in Fig. 1(a). Three unit cells are considered with a total length $2 \times 3 = 6$ mm. Results from the three models are in good agreement.

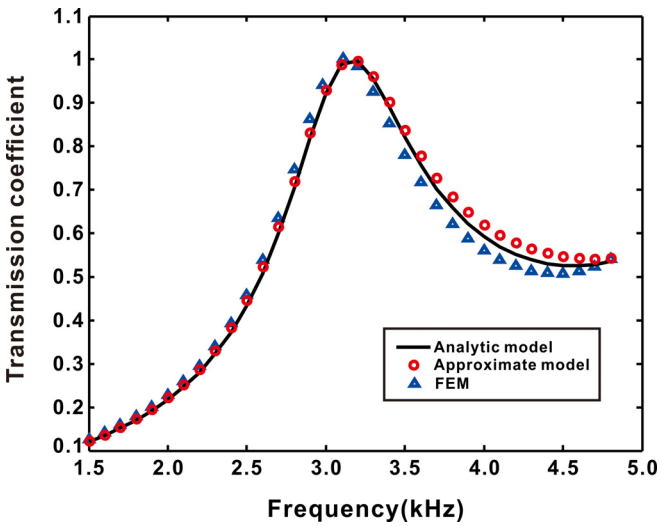

FIG. 9. (Color online) The transmission coefficient of the membrane-type AMM with three unit cells.

IV. CONCLUSION

This paper presents methods for predicting the effective densities of plate- and membrane-type AMMs without mass attached. The analytic model and the approximate model, which is derived from the analytic model under the low frequency approximation, are developed and their results are compared with those from the FEM model. Good agreement is found among these models when predicting the acoustic impedance, effective density, and the transmission coefficients. Although the approximate model is only accurate at frequencies below the first resonance frequency, it provides a quick and reasonably accurate approach for predicting the effective densities of plate- and membrane-type AMMs. The influence of the loss factor of the plate on the effective density and transmission coefficient is investigated. The addition of the loss factor introduces the imaginary part of the effective density and reduces the transmission coefficient. We assume square plates and membranes in this work. The framework we provide, however, can be applied to studying rectangular plates and membranes. Future work will also take the effect of the background medium/fluid into account. This effect is expected to be more significant for plate- and membrane-type AMMs in heavier media, e.g., water.

[1]S. A. Cummer, J. Christensen, and A. Alù, "Controlling sound with acoustic metamaterials," Nat. Rev. Mater. **1**(3), 16001 (2016).
[2]G. Ma and P. Sheng, "Acoustic metamaterials: From local resonances to broad horizons," Sci. Adv. **2**(2), e1501595 (2016).
[3]Z. Liang and J. Li, "Extreme acoustic metamaterial by coiling up space," Phys. Rev. Lett. **108**(11), 114301 (2012).
[4]T. Brunet, A. Merlin, B. Mascaro, K. Zimny, J. Leng, O. Poncelet, C. Aristégui, and O. Mondain-monval, "Soft 3D acoustic metamaterial with negative index," Nat. Mater. **14**, 384–388 (2015).
[5]M. Ambati, N. Fang, C. Sun, and X. Zhang, "Surface resonant states and superlensing in acoustic metamaterials," Phys. Rev. B **75**(19), 195447 (2007).
[6]S. Zhang, C. Xia, and N. Fang, "Broadband acoustic cloak for ultrasound waves," Phys. Rev. Lett. **106**(2), 024301 (2011).
[7]J. J. Park, C. M. Park, K. J. B. Lee, and S. H. Lee, "Acoustic superlens using membrane-based metamaterials," Appl. Phys. Lett. **106**(5), 051901 (2015).
[8]S. Guenneau, A. Movchan, G. Pétursson, and S. Anantha Ramakrishna, "Acoustic metamaterials for sound focusing and confinement," New J. Phys. **9**(11), 399 (2007).
[9]C. Shen, Y. Xie, N. Sui, W. Wang, S. A. Cummer, and Y. Jing, "Broadband acoustic hyperbolic metamaterial," Phys. Rev. Lett. **115**(25), 254301 (2015).
[10]V. M. García-Chocano, J. Christensen, and J. Sánchez-Dehesa, "Negative refraction and energy funneling by hyperbolic materials: An experimental demonstration in acoustics," Phys. Rev. Lett. **112**(14), 144301 (2014).
[11]C. Shen, J. Xu, N. X. Fang, and Y. Jing, "Anisotropic complementary acoustic metamaterial for canceling out aberrating layers," Phys. Rev. X **4**(4), 041033 (2014).
[12]N. Sui, X. Yan, T.-Y. Huang, J. Xu, F.-G. Yuan, and Y. Jing, "A lightweight yet sound-proof honeycomb acoustic metamaterial," Appl. Phys. Lett. **106**(17), 171905 (2015).
[13]Z. Yang, H. M. Dai, N. H. Chan, G. C. Ma, and P. Sheng, "Acoustic metamaterial panels for sound attenuation in the 50–1000 Hz regime," Appl. Phys. Lett. **96**(4), 041906 (2010).
[14]J. Mei, G. Ma, M. Yang, Z. Yang, W. Wen, and P. Sheng, "Dark acoustic metamaterials as super absorbers for low-frequency sound," Nat. Commun. **3**, 756 (2012).
[15]Z. Liu, X. Zhang, Y. Mao, Y. Zhu, and Z. Yang, "Locally resonant sonic materials," Science **289**, 1734–1736 (2000).
[16]Z. Yang, J. Mei, M. Yang, N. Chan, and P. Sheng, "Membrane-type acoustic metamaterial with negative dynamic mass," Phys. Rev. Lett. **101**(20), 204301 (2008).

[17]C. J. Naify, C.-M. Chang, G. McKnight, and S. Nutt, "Transmission loss and dynamic response of membrane-type locally resonant acoustic metamaterials," J. Appl. Phys. **108**(11), 114905 (2010).
[18]C. J. Naify, C.-M. Chang, G. McKnight, F. Scheulen, and S. Nutt, "Membrane-type metamaterials: Transmission loss of multi-celled arrays," J. Appl. Phys. **109**(10), 104902 (2011).
[19]C. M. Park, J. J. Park, S. H. Lee, Y. M. Seo, C. K. Kim, and S. H. Lee, "Amplification of acoustic evanescent waves using metamaterial slabs," Phys. Rev. Lett. **107**(19), 194301 (2011).
[20]S. H. Lee, C. M. Park, Y. M. Seo, Z. G. Wang, and C. K. Kim, "Acoustic metamaterial with negative density," Phys. Lett. A **373**(48), 4464–4469 (2009).
[21]S. H. Lee, C. M. Park, Y. M. Seo, Z. G. Wang, and C. K. Kim, "Composite acoustic medium with simultaneously negative density and modulus," Phys. Rev. Lett. **104**(5), 054301 (2010).
[22]S. Yao, X. Zhou, and G. Hu, "Investigation of the negative-mass behaviors occurring below a cut-off frequency," New J. Phys. **12**(10), 103025 (2010).
[23]Y. Jing, J. Xu, and N. X. Fang, "Numerical study of a near-zero-index acoustic metamaterial," Phys. Lett. A **376**(45), 2834–2837 (2012).
[24]J. J. Park, K. J. B. Lee, O. B. Wright, M. K. Jung, and S. H. Lee, "Giant acoustic concentration by extraordinary transmission in zero-mass metamaterials," Phys. Rev. Lett. **110**(24), 244302 (2013).
[25]R. Fleury and A. Alù, "Extraordinary sound transmission through density-near-zero ultranarrow channels," Phys. Rev. Lett. **111**(5), 055501 (2013).
[26]X. Zhou and G. Hu, "Superlensing effect of an anisotropic metamaterial slab with near-zero dynamic mass," Appl. Phys. Lett. **98**(26), 263510 (2011).
[27]A. Liu and X. Zhou, "Super-resolution imaging by resonant tunneling in anisotropic acoustic metamaterials," J. Acoust. Soc. Am. **132**(4), 2800–2806 (2012).
[28]F. Bongard, H. Lissek, and J. R. Mosig, "Acoustic transmission line metamaterial with negative/zero/positive refractive index," Phys. Rev. B **82**(9), 094306 (2010).
[29]C.-C. Sung and J. T. Jan, "The response of and sound power radiated by a clamped rectangular plate," J. Sound Vib. **207**, 301–317 (1997).
[30]W. Leissa, *Vibration of Plates* (NASA, Washington, DC, 1969), Chap. 4.
[31]Y. Cheng, J. Y. Xu, and X. J. Liu, "One-dimensional structured ultrasonic metamaterials with simultaneously negative dynamic density and modulus," Phys. Rev. B **77**(4), 045134 (2008).
[32]C. Shen and Y. Jing, "Side branch-based acoustic metamaterials with a broad-band negative bulk modulus," Appl. Phys. A **117**(4), 1885–1891 (2014).
[33]S. H. Lee and O. B. Wright, "Origin of negative density and modulus in acoustic metamaterials," Phys. Rev. B **93**(2), 024302 (2016).
[34]L. E. Kinsler, A. R. Frey, A. B. Coppens, and J. V. Sanders, *Fundamentals of Acoustics*, 4th ed. (Wiley, Hoboken, NJ, 2000), pp. 92–94.